Improving perfusion defect detection with respiratory motion correction in cardiac SPECT at standard and reduced doses

Chao Song, MS,[a] Yongyi Yang, PhD,[a] Albert Juan Ramon, MS,[a] Miles N. Wernick, PhD,[a] P. Hendrik Pretorius, PhD,[b] Karen L. Johnson, BS,[b] Piotr J. Slomka, PhD,[c] and Michael A. King, PhD[b]

[a] Medical Imaging Research Center, Illinois Institute of Technology, Chicago, IL
[b] Department of Radiology, University of Massachusetts Medical School, Worcester, MA
[c] Department of Medicine, Cedars-Sinai Medical Center, Los Angeles, CA

Received Mar 25, 2018; accepted May 11, 2018
doi:10.1007/s12350-018-1374-9

Background. **In cardiac SPECT perfusion imaging, respiratory motion can cause non-uniform blurring in the reconstructed myocardium. We investigate the potential benefit of respiratory correction with respiratory-binned acquisitions, both at standard dose and at reduced dose, for defect detection and for left ventricular (LV) wall resolution.**

Methods. **We applied two reconstruction methods for respiratory motion correction: post-reconstruction motion correction (PMC) and motion-compensated reconstruction (MCR), and compared with reconstruction without motion correction (Non-MC). We quantified the presence of perfusion defects in reconstructed images by using the total perfusion deficit (TPD) scores and conducted receiver-operating-characteristic (ROC) studies using TPD. We quantified the LV spatial resolution by using the FWHM of its cross-sectional intensity profile.**

Results. **The values in the area-under-the-ROC-curve (AUC) achieved by MCR, PMC, and Non-MC at standard dose were 0.835, 0.830, and 0.798, respectively. Similar AUC improvements were also obtained by MCR and PMC over Non-MC at 50%, 25%, and 12.5% of full dose. Improvements in LV resolution were also observed with motion correction.**

Conclusions. **Respiratory-binned acquisitions can improve perfusion-defect detection accuracy over traditional reconstruction both at standard dose and at reduced dose. Motion correction may contribute to achieving further dose reduction while maintaining the diagnostic accuracy of traditional acquisitions. (J Nucl Cardiol 2019;26:1526–38.)**

Spanish Abstract

Antecedentes. **En los estudios de perfusión cardiaca por SPECT, los movimientos respiratorios pueden causar distorsión no uniforme en el miocardio reconstruido. Investigamos el beneficio potencial de la corrección respiratoria con adquisición de imágenes sincronizadas con**

Electronic supplementary material The online version of this article (https://doi.org/10.1007/s12350-018-1374-9) contains supplementary material, which is available to authorized users.

The authors of this article have provided a PowerPoint file, available for download at SpringerLink, which summarises the contents of the paper and is free for re-use at meetings and presentations. Search for the article DOI on SpringerLink.com.

This article is accompanied by an .mp3 audio interview, available for download from the article's SpringerLink page under 'Supplementary material', and also at the 'JNC/ASNC Podcast'. The interview was held between Yongyi Yang and Heinrich R. Schelbert on 11th June 2018.

JNC thanks Erick Alexanderson MD, Carlos Guitar MD, and Diego Vences MD, UNAM, Mexico, for providing the Spanish abstract; Zhuo He BS, Haipeng Tang MS, Zhixin Jiang MD, and Weihua Zhou PhD, for providing the Chinese abstract; and Jean-Luc Urbain, MD, PhD, CPE, Past President CANM, Chief Nuclear Medicine, Lebanon VAMC, PA, for providing the French abstract.

Reprint requests: Yongyi Yang, Medical Imaging Research Center, Illinois Institute of Technology, 3440 S. Dearborn St., Suite 100, Chicago, IL 60616; *yangyo@iit.edu*

1071-3581/$34.00

la respiración, tanto a dosis estándar como a dosis reducida, para detección de defectos y para resolución de pared de ventrículo izquierdo (VI).

Métodos. **Aplicamos dos métodos de reconstrucción para corrección de movimientos respiratorios: Corrección de movimiento post reconstrucción (PMC) y reconstrucción compensada a movimiento (MCR), y los comparamos con la reconstrucción sin corrección de movimiento (Non-MC). Cuantificamos la presencia de defectos de perfusión en las imágenes reconstruidas usando los scores de déficit total de perfusión (TPD) y análisis ROC usando el TPD. Cuantificamos la resolución espacial del VI usando la anchura a media altura de su perfil de intensidad transversal.**

Resultados. **Los valores en el área bajo la curva ROC (ABC) obtenidos por MCR, PMC y Non-MC a dosis estándar fueron 0.835, 0.830 y 0.798, respectivamente. Mejorías similares del ABC también se obtuvieron por MCR y PMC, sobre Non-MC a 50%, 25% y 12.5% de la dosis completa. Las mejorías en la resolución del VI fueron observadas también con corrección del movimiento.**

Conclusiones. **Las adquisiciones sincronizadas con la respiración pueden mejorar la precisión de la detección de defectos de perfusión sobre las reconstrucciones tradicionales tanto a dosis estándar como a dosis reducida. La corrección de movimiento puede contribuir a lograr mayor reducción de la dosis manteniendo la precisión diagnóstica de las adquisiciones tradicionales. (J Nucl Cardiol 2019;26:1526–38.)**

Chinese Abstract

背景. 在心脏 SPECT 灌注成像中, 呼吸运动会导致心肌重建的不均匀模糊。我们研究了无论是标准剂量还是减少剂量的情况下, 呼吸跟踪采集的呼吸校正用于图像缺损检测和左心室 (LV) 室壁分辨率的潜在益处。

方法. 我们使用了两种呼吸运动校正的重建方法:重建后运动校正 **(PMC)** 和运动补偿重建 **(MCR),** 并与没有运动校正的重建 **(Non-MC)** 进行比较。 通过总灌注缺损 **(TPD)** 评分和其接受者操作特性曲线 **(ROC)** 来量化重建图像中的灌注缺陷。通过**LV**横截面强度分布的 **FWHM**来量化 **LV** 空间分辨率。

结果. **MCR, PMC** 和 **Non-MC** 在标准剂量下所获得的 **ROC** 曲线下面积 **(AUC)** 的值分别为**0.835, 0.830** 和 **0.798**。 在全剂量下**, MCR, PMC**和 **Non-MC** 也获得类似的 **AUC** 提高,分别为 **50%, 25%** 和 **12.5%**。 在运动校正下, **LV**的分辨率也得到了改善。

结论. 在标准剂量和减少剂量的情况下,呼吸跟踪采集可以改善灌注缺损检测的准确性。运动校正可能有助于进一步实现减少剂量的目标, 同时保证通过传统检测方法的诊断准确性。**(J Nucl Cardiol 2019;26:1526–38.)**

French Abstract

Contexte. **Les mouvements respiratoires peuvent entrainer des artefacts de uniformité lors de la reconstruction des images de perfusion myocardique en SPECT. Dans cet article, nous rapportons nos résultats sur le bénéfice potentiel du « gating » respiratoire avec des doses standards et réduites de radio-pharmaceutiques pour la détection des anomalies de perfusion et les mesures de la paroi ventriculaire gauche.**

Méthodes. **Nous avons appliqué deux méthodes de reconstruction pour la correction du mouvement respiratoire: la première fait appel a une correction après reconstruction des images (PMC) ; la seconde fait appel à la correction des images avant reconstruction (MRC). Les deux approches ont été comparées à la reconstruction sans correction de mouvement (Non-MC). Nous avons quantifié les déficits de perfusion myocardiques sur les images reconstruites avec le système des scores de déficit de perfusion et analysé les résultats en utilisant les courbes ROC. Nous avons quantifié la résolution spatiale du VG en utilisant le FWHM du profil d'intensité de sa section transversale.**

Résultats. **Les valeurs des surfaces en dessous des courbes ROC (AUC) obtenues par MCR, PMC et Non-MC avec doses standard de radio-pharmaceutiques étaient de 0,835, 0,830 et 0,798, respectivement. Des améliorations similaires de l'AUC ont également été obtenues par MCR et PMC sur Non-MC avec 50%, 25% et 12,5% des doses entières. Les mesures de résolution**

spatiale de la paroi du VG ont également été améliorées avec la correction des mouvements respiratoires.

Conclusions. **La correction des images de perfusion myocardiques en SPECT par « gating » respiratoire paraît améliorer la quantification des déficits perfusionels à la fois à dose standard et à dose réduite de radio-pharmaceutiques. L'application de cette correction devrait permettre de réduire les doses de radio-pharmaceutiques utilisées tout en maintenant la précision diagnostique des acquisitions traditionnelles.**

Key Words: CAD · SPECT · MPI · image reconstruction

Abbreviations	
SPECT	Single-photon emission computed tomography
TPD	Total perfusion deficit
QPS	Quantitative Perfusion SPECT
AUC	Area under the ROC curve
FWHM	Full-width at half-maximum
LV	Left ventricle
MCR	Motion-compensated reconstruction
PMC	Post-reconstruction motion correction
MPI	Myocardial perfusion imaging
BSREM	Block-sequential regularized expectation-maximization
OSEM	Ordered-subset expectation-maximization
ROC	Receiver operating characteristic

INTRODUCTION

Myocardial perfusion imaging (MPI) with single-photon emission computed tomography (SPECT) can provide important diagnostic information about myocardial perfusion and ventricular function,[1] which allows for evaluation and quantification of the extent and severity of myocardial hypoperfusion and ischemia.[2-4] The image quality in cardiac SPECT can be degraded by a number of factors,[5] e.g., imaging noise, limited resolution, motion blur, etc. Respiratory motion is known to cause non-uniform blurring in MPI, which may negatively affect the diagnostic accuracy.[6,7] There have been simulation and experimental studies reported on the effects of respiratory motion, upward creep, and respiratory hysteresis on the image quality.[8-10] An effective strategy for reducing the extent of motion blur is to use respiratory-binned acquisitions,[11,12] which can be achieved by phase binning or amplitude binning.[13]

In this study, we investigate the benefit of respiratory motion correction in the clinical task of defect detection. Previous studies show that image reconstruction with respiratory-binned data can lead to improved image accuracy based on figures-of-merit such as mean-squared-error and image resolution.[14,15] Our purpose herein is to study quantitatively how such improved reconstruction accuracy may translate to perfusion defect detection in clinical acquisitions. From our past experience, there can be a large degree of both intra- and inter-subject variability in respiratory patterns from the patient population, which can cause great variability in data statistics among respiratory bins and projection angles with a conventional rotating SPECT system.[14,16] Thus, to reflect the extent of biological variability observed clinically, for this study we used clinical acquisitions rather than simulated phantom data. For motion correction, we considered two reconstruction methods: (1) post-reconstruction motion correction (PMC), in which the individual respiratory bins are reconstructed separately and combined with motion correction subsequently[15] and (2) motion-compensated reconstruction (MCR), in which data from different respiratory bins are applied simultaneously for reconstructing the source image with respect to a common reference bin.[14,17]

In addition, in this study we also investigate the benefit of respiratory correction with reduced dose in SPECT-MPI. In recent years there have been growing interests in reducing the imaging dose for cardiac SPECT.[18-25] In our experiments, we also quantified the reconstruction results when the imaging dose was reduced to 50% (one half), 25% (one quarter), and 12.5% (one eighth) of full acquisitions.

To quantify the accuracy for perfusion defect detection, we conducted a receiver-operating characteristic (ROC) study based on hybrid studies, i.e., clinical data in which simulated defects were introduced, as in Ref. 26. The reconstructed images were evaluated by the total perfusion deficit (TPD) scores for quantifying the presence of perfusion defects, as computed by the Quantitative Perfusion SPECT (QPS) software package (a clinical model observer extensively validated in past studies).[4] We then used the TPD scores to obtain the defection performance, as measured by the area under the ROC curve (AUC). In addition, we also examined the improvement in image resolution of the reconstructed left ventricle (LV) upon motion correction, for which we computed the full-width at half-maximum (FWHM) of the intensity profile across the midsection of the LV.

Table 1. Clinical characteristics of the patient population used in this study

	Male subjects ($n = 71$)	Female subjects ($n = 119$)
1. Body mass index (kg m^{-2})	30.4 ± 5.4	30.0 ± 5.5
2. Age (years)	56.8 ± 13.4	63.1 ± 11.0
3. Extent of superoinferior motion (cm)	0.90 ± 0.36	0.89 ± 0.34
4. Effective injected activity (MBq)	1180 ± 144	1188 ± 137

The first three quantities were obtained from all the 190 subjects, whereas the last quantity was obtained from 121 subjects for which the data was available for this study. The effective injected activity was calculated from the initial activity in the syringe corrected for the post-injection activity left in the syringe and half-life decay. The extent of respiratory motion was determined from the displacement magnitude between the two extreme bins in the respiratory cycle

MATERIALS AND METHODS

Data Acquisition

We studied SPECT-MPI data of consecutive 190 patients (71/119, male/female) who gave written consent to participate in our investigations, had no technical issues in their acquisitions, and were interpreted as having normal perfusion. These studies were stress imaging acquired on a Philips BrightView SPECT/CT system in list-mode with Tc-99m sestamibi and a visual tracking system from 2013 to 2016 at the University of Massachusetts Medical School. This data set was also used in our previous study[26] for the purpose of optimizing reconstruction algorithms, where a detailed description of the acquisition parameters and patient characteristics was given. In this study, we investigate the effect of respiratory motion correction. For this purpose, the list-mode data were rebinned into seven respiratory intervals based on the respiratory amplitude signal recorded by a visual tracking system (Vicon Motion Systems, Inc., Lake Forest, CA) during acquisitions as previously detailed.[16] A summary of the clinical attributes of the 190 patients is given in Table 1.

For perfusion defect detection, 60 studies (30 male, 30 female) among the 190 patients were allocated for the formation of reference databases in QPS, while the remaining 130 patients were used for the ROC study as in Ref. 26. The patients in the data set exhibited various degrees of respiratory motion (Table 1); the allocation of study patients was blind to the magnitude of their respiratory motion. Among the 130 study patients, 72 were used for inserting perfusion defects in order to provide ground truth for the ROC study[27]; these "hybrid studies" were created from the acquired data of the 72 subjects in which realistic perfusion defects were introduced randomly (with equal probability) among the left-anterior-descending coronary artery (LAD), the right coronary artery (RCA), and the left circumflex (LCX) vascular territories. They could contain one- or two-vessel disease with their locations and sizes selected according to clinical prevalence.[28] The extents of the defects were also varied randomly with different sizes among the subjects (large: 20.06 ± 5.13 g; moderate: 10.99 ± 2.98 g; small: 7.98 ± 3.32 g). To further reflect the variability in clinical studies, each defect was also introduced with four contrast levels (65%, 50%, 35%, and 20%). The contrast level is the reduction in count-density relative to normal regions.

Furthermore, to assess the reconstruction with reduced dose imaging, we applied a statistical resampling procedure[19,26] to the acquisitions of the 190 subjects at full dose (100%) and obtained data at the following reduced dose levels: 50%, 25%, and 12.5%. With this procedure, the individual photon events acquired in list-mode at 100% dose were randomly accepted or rejected according to a binomial trial probability of 1/2, 1/4, and 1/8, respectively, resulting in acquisitions for the same duration but respective reduction in the administered dose.

Reconstruction Methods

For motion correction, we considered the following two reconstruction methods: (1) post-reconstruction motion correction (PMC), wherein motion correction is applied after the images are first obtained from the individual respiratory bins,[15,17] and (2) motion-compensated reconstruction (MCR), wherein the projection data from the different respiratory bins are used simultaneously for reconstruction of the source distribution with respect to a reference bin through motion compensation.[17] The specific steps involved in these two reconstruction methods are as follows:

a. PMC method

Step 1 Reconstruct image $\mathbf{f}_r$ from the acquired data in each respiratory bin r, $r = 1, \ldots, R$;

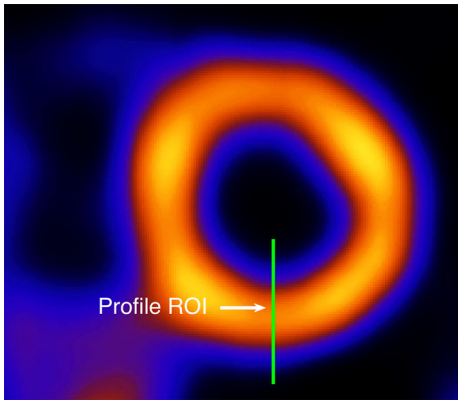

Figure 1. A mid-LV short-axis slice illustrating the inferior wall location used for image intensity profile analysis. The full-width at half-maximum (FWHM) of the image intensity profile is used to quantify the LV resolution.

Step 2 Estimate the image motion from each bin r to a common reference bin r_0 based on their reconstructed images;
Step 3 Combine the images $\mathbf{f}_r$ from different bins with respect to the reference bin r_0 based on their image motion.
The details of these steps are described in Refs. 15,17.

b. MCR method

Step 1 Pre-reconstruct image $\mathbf{f}_r$ from the acquired data in each respiratory bin r, $r = 1, \ldots, R$;
Step 2 Estimate the image motion from bin r to a common reference bin r_0 based on their pre-reconstructed images;
Step 3 Express image $\mathbf{f}_r$ in each bin in terms of the reference bin $\mathbf{f}_{r_0}$ based on their image motion, and reconstruct the image $\mathbf{f}_{r_0}$ from the acquired data in all the respiratory bins simultaneously.
The details of these steps can be found in Ref.17.

Herein $R = 7$ respiratory bins based on the amplitude of the superoinferior motion were used and the reference bin was the center bin ($r_0 = 4$). In addition, for comparison, we also considered reconstruction with conventional acquisition, i.e., without respiratory binning (denoted by Non-MC). In all these methods, namely PMC, MCR and Non-MC, the effects of attenuation, depth dependent blur, and scatter were all accounted for Ref.16. For scatter correction, the triple energy window (TEW) method[29] was used. For attenuation correction, the attenuation maps were acquired from flat panel cone-beam CT imaging under normal patient breathing prior to SPECT acquisition.[16]

To compensate for the variation in data counts among projection angles and respiratory bins associated with respiratory-binned data, a time factor was introduced into the imaging model as in Ref. 17. This time factor was used to account for the actual acquisition time at a particular projection angle and respiratory bin, which is available from the list-mode data. This was demonstrated to be effective for suppressing the presence of limited-angle effect in the respiratory-binned images due to the uneven nature of respiratory motion.[17]

In all three reconstruction methods PMC, MCR, and Non-MC, maximum likelihood (ML) estimation was used to obtain the image from the projection data (binned from list-mode). We used the modified block-sequential regularized expectation-maximization (BSREM) algorithm.[30] This algorithm has the property of global convergence, and was demonstrated to achieve improved image quality and lesion detectability.[30,31] In our experiments, a total of 16 ordered subsets and 10 iterations were used based on our previous studies.[17,19]

To suppress the noise effect, we further applied 3D Gaussian filtering to the reconstructed images. The smoothing level was controlled through the width parameter Sigma of the Gaussian kernel. With this approach, one can easily adjust the level of smoothing without the need to rerun the reconstruction algorithm. As the noise gets increased with reduced dose acquisition, more smoothing (i.e., larger Sigma value) is expected to be needed. In the experiments, we optimized the parameter Sigma for improving the accuracy in lesion detection for each reconstruction method and at each dose level. The following Sigma values (in voxels) were used: 0.8, 1, 1.2, 1.5, and 2.

As in Refs. 15,17, a 3D translational model was used for the image motion among different respiratory bins, where the motion was estimated from the individual bins using a template-matching algorithm.[32] A bounding box was first extracted to contain the LV in the reference bin. This bounding box was then used as a template to determine its correspondence in other respiratory bins. Translational motion was previously determined to be effective for respiratory correction in cardiac SPECT given its limited spatial resolution.[12]

Assessment of Reconstructed Images

To assess the reconstruction results, we used the following two quantitative measures: detectability of perfusion defect in the reconstructed myocardium, and the spatial resolution of the LV wall. These two measures were used together to demonstrate how respiratory correction can reduce the image blur and improve the defect detectability.

For perfection defect detection, we used the total perfusion deficit (TPD) score of the Quantitative Perfusion SPECT (QPS) package (Cedars-Sinai).[3] The TPD is

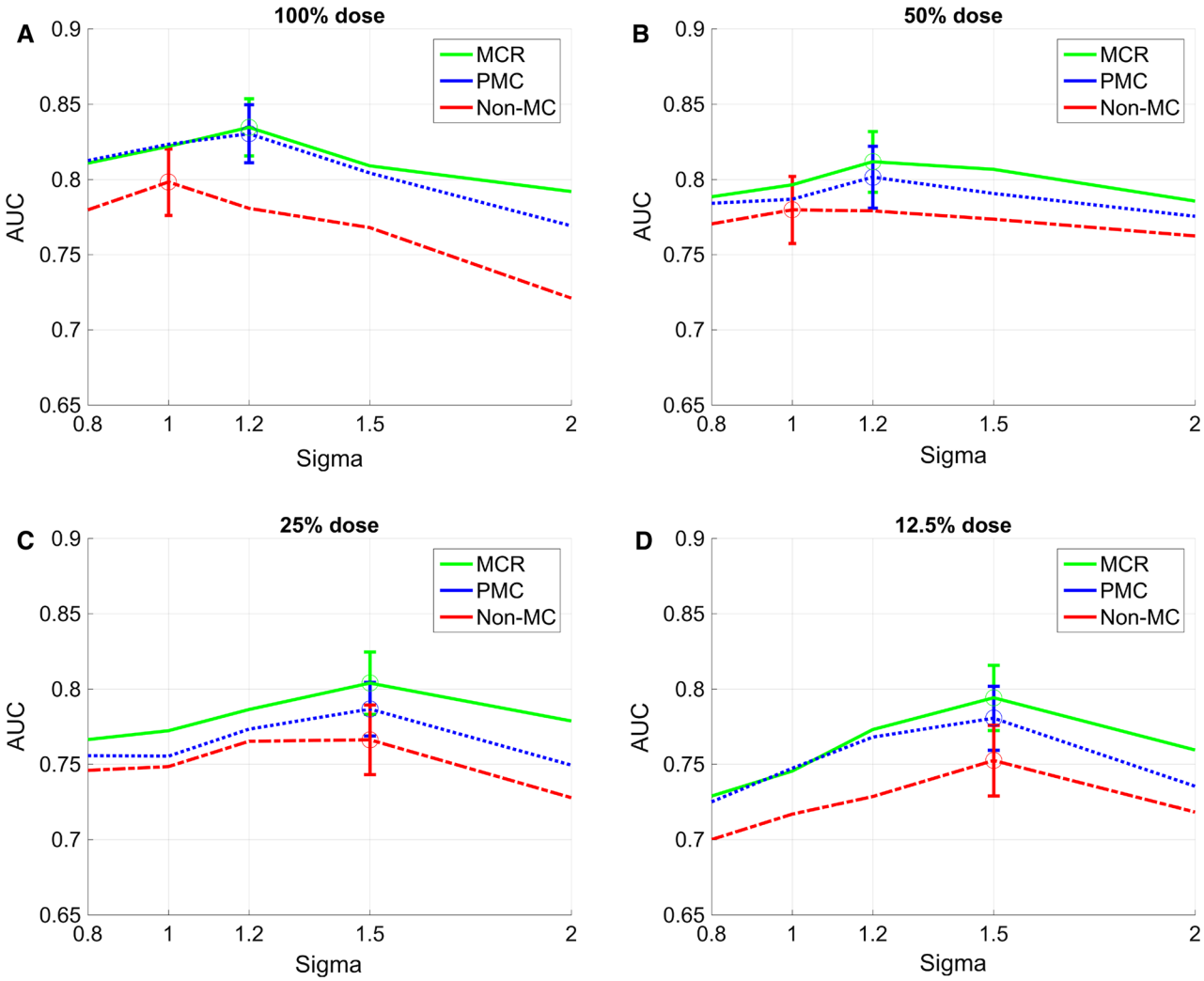

Figure 2. Perfusion defect detection results, measured by AUC, obtained at various dose levels: (**A**) 100%, (**B**) 50%, (**C**) 25%, and (**D**) 12.5%. The reconstruction methods are: motion-compensated reconstruction (MCR), post-reconstruction motion correction (PMC), and no motion correction (non-MC). The AUC value is plotted vs the width parameter Sigma of the 3D Gaussian filter (larger Sigma value corresponding to more smoothing). The circle marker on each curve indicates the optimal (maximum) AUC value for the corresponding reconstruction method. The error bars correspond to ± 1 SD.

a summary measure of the non-uniformity of myocardium perfusion, with TPD scores defined in accordance with the severity and extent of the defects present.[4] For ROC assessment, the TPD values were input into Metz's ROCKIT software[33] to obtain the detection performance from the reconstructed images, which was summarized by the area under the ROC curve (AUC); a larger AUC value corresponds to better detection accuracy. The ROCKIT software was also used to determine the statistical difference in detection performance between reconstruction methods.

For the normal reference databases in QPS, we used a set of 60 patients (30 males and 30 females).[4] These subjects were reconstructed for each of the different settings of the reconstruction algorithm used, patient gender, and the imaging dose level. Therefore, for example, a male subject reconstructed at half dose by the MCR algorithm with smoothing parameter Sigma $= 1.0$ was quantified by the reference database reconstructed with exactly the same setting.

For quantifying the LV wall resolution, we computed the full-width at half-maximum (FWHM) of the image intensity profile for a cross-section in the reconstructed LV (Figure 1). The improvement in the spatial resolution upon motion correction is expected to lead to smaller FWHM values in the reconstructed LV.[34] The

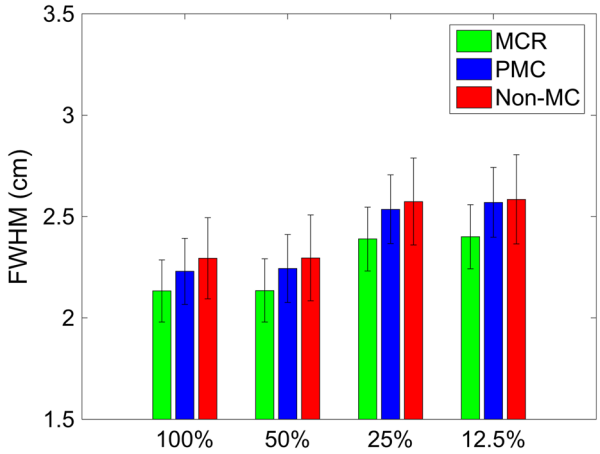

Figure 3. FWHM values of the reconstructed LV wall counts (at location shown in Figure 1) at various dose levels (i.e. 100%, 50%, 25%, and 12.5%). The reconstruction methods are: motion-compensated reconstruction (MCR), post-reconstruction motion correction (PMC), and no motion correction (Non-MC). The error bars denote ±1 SD. Note the increase in FWHM with decreased dose due to the larger smoothing applied (as per Figure 2).

paired sample *t*-test was used to compare the statistical difference in FWHM between two reconstruction methods. For each reconstruction method, the smoothing parameter Sigma was set according to the optimal AUC results at the different dose levels.

RESULTS

Perfusion Defect Detection Performance

In Figure 2A we show the ROC results on perfusion-defect detection obtained from the full dose data by reconstruction methods MCR, PMC, and Non-MC. In the figure, each curve denotes the AUC value by one reconstruction method with different smoothing levels. Note that both MCR and PMC obtained higher AUC values (hence better detection) than Non-MC at each of the smoothing levels. In particular, MCR achieved the best AUC = 0.835 (Sigma = 1.2), compared to 0.798 for Non-MC (Sigma = 1.0) (P value = 0.0001); for PMC the best AUC = 0.830 (Sigma = 1.2), also higher than Non-MC (P value = 0.003).

Similarly, in Figure 2B-D we show the ROC results obtained from the reduced dose data of 50%, 25%, and 12.5% of full dose, respectively. At each reduced dose, both MCR and PMC achieved higher AUC values than Non-MC. Specifically, at 50% dose, the best AUC values by MCR, PMC, and Non-MC are 0.812, 0.801, and 0.780, respectively; at 25% dose, their best AUC values are 0.804, 0.787, and 0.766, respectively; at 12.5% dose, their best AUC values are 0.794, 0.781, and 0.753, respectively. At each reduced dose, both MCR and PMC outperformed Non-MC (P value < 0.05).

The ROC results in Figure 2 indicate that respiratory motion correction can consistently provide better defect detection performance both at full dose and at reduced dose. Between the two methods, MCR yielded slightly higher AUC values than PMC (P value < 0.05 at all dose levels except for full dose). Remarkably, at both 50% and 25% dose levels, the AUC values achieved by MCR are higher than Non-MC at 100% dose. Even at 12.5% dose, the AUC of MCR (0.794) is only marginally lower than the AUC of 0.798 by Non-MC at 100% dose (P value = 0.11).

FWHM Evaluation

In Figure 3 we show a plot of the FWHM values obtained by the three reconstruction methods MCR, PMC, and Non-MC both at full dose and at reduced dose (i.e., 100%, 50%, 25%, and 12.5%). These results were obtained from the average of 118 normal subjects (hybrid cases excluded) in the dataset.

The results in Figure 3 indicate that at all dose levels MCR and PMC could yield smaller FWHM values (hence less motion blur and better image resolution) than Non-MC. At full dose, the FWHM values are 2.13, 2.23, and 2.29 cm for MCR, PMC, and Non-MC, respectively; P value = 0.009 between MCR and Non-MC, and P value = 0.02 between PMC and Non-MC. Similar improvements were also obtained in the reduced dose data. For example, at 25% dose, the FWHM values are 2.39, 2.54, and 2.57 cm for MCR, PMC, and Non-MC, respectively. It is also observed from Figure 3 that the FWHM values show a monotonic increase for each reconstruction method as the imaging dose reduced. This is due to the increased spatial smoothing (larger Sigma values) for optimizing the lesion detection in response to the increased noise in reduced dose.

Reconstructed Images at Full Dose

In Figure 4, we show a set of reconstructed images obtained for a normal female subject #1 (age: 59, BMI: 42.5) at 100% dose. The images in Figure 4A are short-axis slices (and polar maps) from each of the three methods: MCR (1st row), PMC (2nd row), and Non-MC (3rd row); similarly, the long-axis slices are shown in Figure 4B. In these images the smoothing parameter was set according to the optimal AUC results for each method.

From these images the LV wall is noted to be more uniform in both MCR and PMC than in Non-MC. The

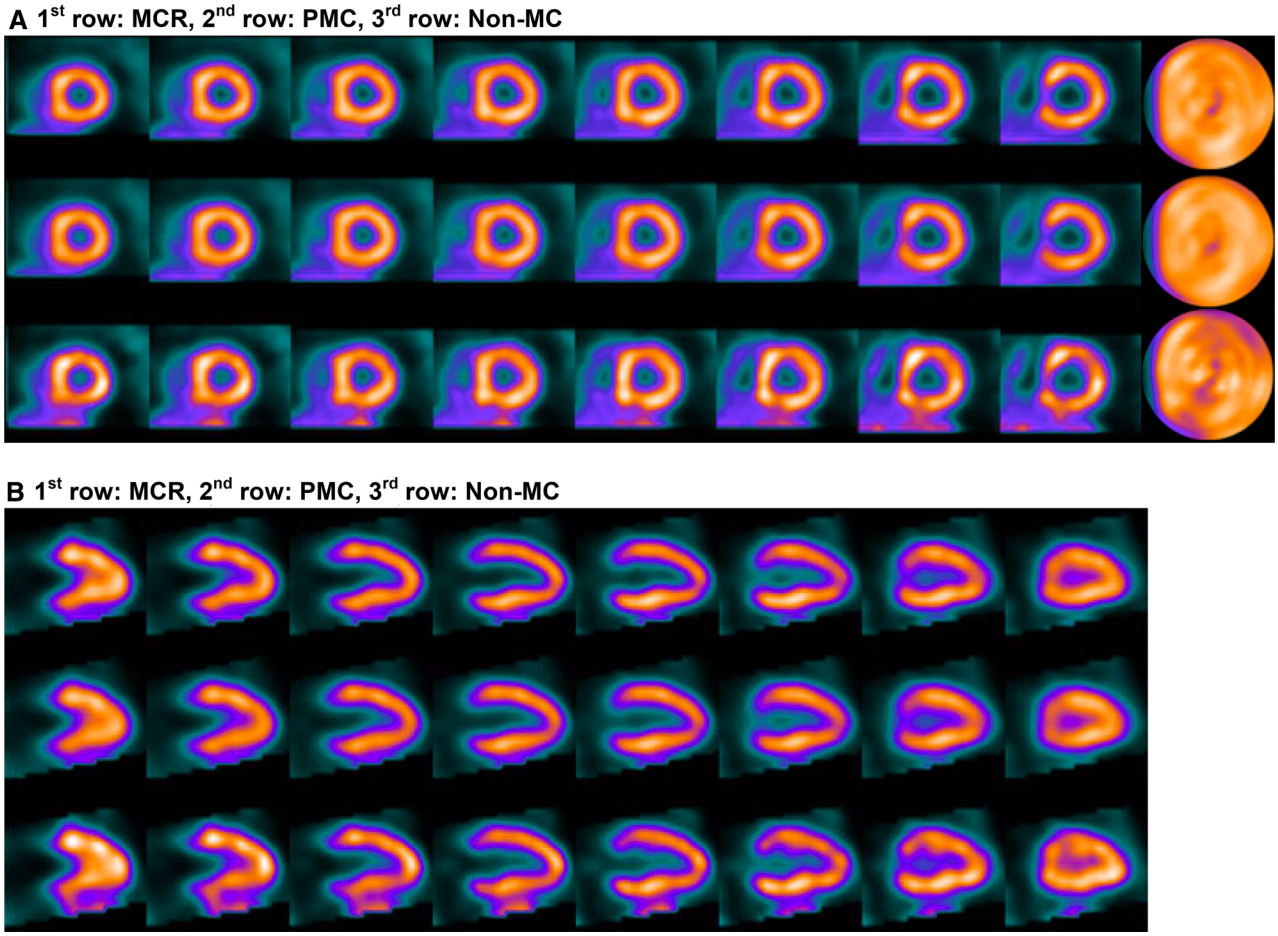

Figure 4. Reconstructed images (**A** short-axis slices and polar maps; **B** vertical long-axis slices) from the clinical data of subject #1 (female, age: 59, BMI: 42.5) at 100% dose. The extent of superoinferior motion of the LV due to respiratory motion was 1.87 cm. The results are shown in (**A**) and (**B**) for each of the three reconstruction methods: motion-compensated reconstruction (MCR) (1st row), post-reconstruction motion correction (PMC) (2nd row), and no motion correction (Non-MC) (3rd row). The cooling artifact observed in anterior and inferior LV walls in Non-MC is improved by respiratory motion correction in MCR and PMC. There is also better separation in LV from sub-diaphragmatic activity in MCR and PMC.

cooling artifact (i.e., decreased count-density) in the anterior and inferior walls in Non-MC is notably improved with respiratory motion correction in MCR and PMC. This is particularly evident from the polar maps. Moreover, the LV wall also appears less blurry in both MCR and PMC than in Non-MC. This is consistent with the improvement in spatial resolution by MCR and PMC earlier in Figure 3. In addition, "spill-over" from sub-diaphragmatic bowel activity near the LV wall is observed in the Non-MC images, but suppressed in both MCR and PMC.

In Figure 5, we show a set of reconstructed images obtained for a male subject #2 (age: 53, BMI: 22.0) at 100% dose. In this study there was a moderate sized defect with 50% contrast introduced in the RCA territory (indicated by the arrows). It can be observed that the LV wall (aside from the defect) is more uniform in both MCR and PMC than in Non-MC; the cooling artifact in the normal region of the inferior LV wall in Non-MC is improved in MCR and PMC.

Reconstructed Images at Reduced Dose

In Figures 6 and 7, we show the reconstructed images from the reduced dose data of the same two subjects earlier in Figures 4 and 5; for each subject, the images were obtained at only 12.5% of full dose. In these images, the smoothing parameter was set according to the optimal AUC results (i.e., Sigma = 1.5).

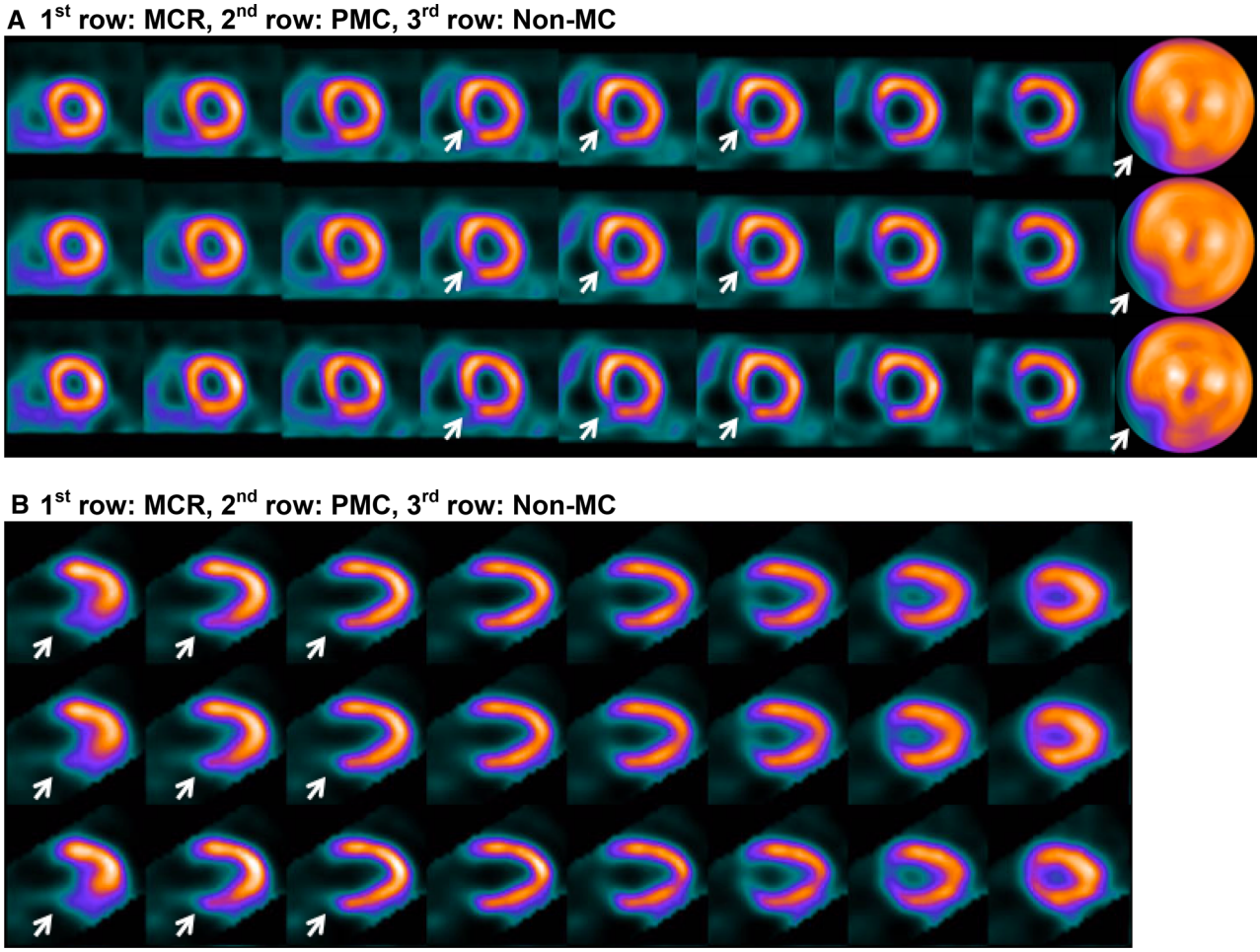

Figure 5. Reconstructed images (**A**: short-axis slices and polar maps; **B**: vertical long-axis slices) of subject #2 (male, age: 53, BMI: 22.0) at 100% dose. There was a moderate sized defect with 50% contrast (green arrows) introduced in the RCA territory. The extent of superoinferior motion of the LV due to respiratory motion was 1.28 cm. The results are shown in (**A**) and (**B**) for each of the three reconstruction methods: motion-compensated reconstruction (MCR) (1st row), post-reconstruction motion correction (PMC) (2nd row), and no motion correction (Non-MC) (3rd row). The regional cooling away from the defect in the inferior LV wall observed in Non-MC is reduced by respiratory motion correction in MCR and PMC.

Compared to their counterparts in Figures 4 and 5, the images in Figures 6 and 7 appear to be slightly more blurry (due to increased smoothing). Nevertheless, the image improvements by MCR and PMC over Non-MC remain consistent with that observed in the full dose. The LV wall is noted to be more uniform and less blurry in MCR and PMC than in Non-MC. The regional cooling observed in anterior and inferior LV walls in Non-MC is notably suppressed in MCR and PMC. The sub-diaphragmatic activity observed in patient #1 with Non-MC is also better separated in the reconstructed LV with MCR and PMC.

DISCUSSION

There have been a number of recent studies on optimizing reconstruction strategies for reducing the imaging dose in SPECT-MPI.[25,26,35] To our best knowledge, this study is the first to investigate the potential benefit of respiratory correction for the task of perfusion defect detection when the imaging dose is successively reduced from full acquisitions. We considered two reconstruction algorithms for motion correction, post-reconstruction motion correction (PMC) and motion-compensated reconstruction (MCR). Compared to

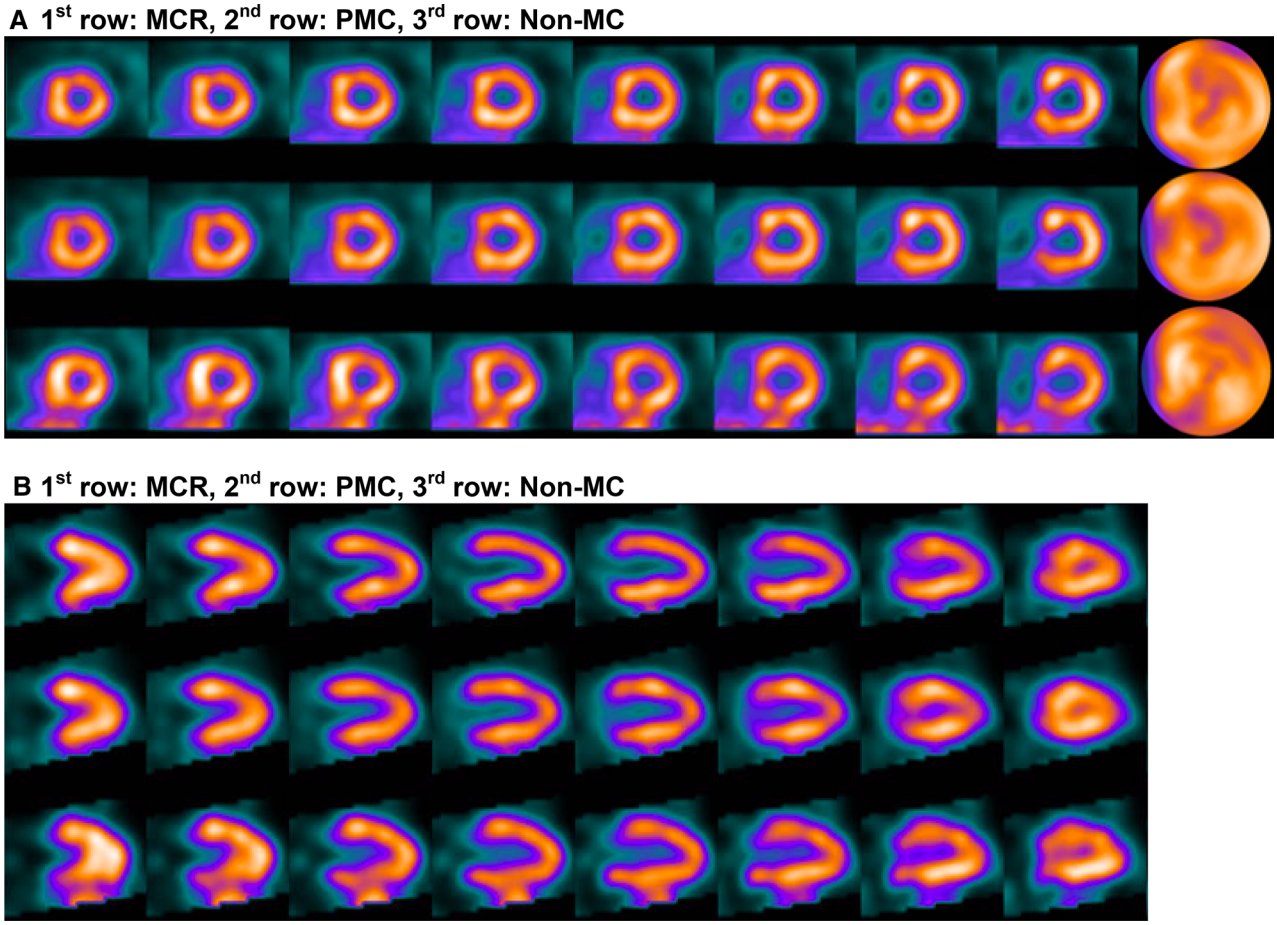

Figure 6. Reconstructed images from the clinical data of subject #1 (same as in Figure 4) at 12.5% dose. The regional cooling observed in anterior and inferior LV walls in Non-MC is improved by respiratory motion correction in MCR and PMC. There is also better separation in LV from sub-diaphragmatic activity in MCR and PMC.

traditional acquisitions, both MCR and PMC achieved higher AUC values for defect detection at all dose levels. MCR also outperformed PMC by a small margin, with the differences increasingly larger at lower dose levels. For example, at full dose, the AUC values are 0.835 (MCR) and 0.830 (PMC); at 12.5% dose, the AUC values are 0.794 (MCR) and 0.781 (PMC). These results suggest that MCR can be more robust to the increased noise level than PMC.

Respiratory motion is known to cause non-uniform blurring in MPI. This is observed in the reconstructed images in Figures 4, 5, 6, and 7 at different dose levels, wherein the reconstructed LV exhibited perfusion variations (hence reduced uniformity) when no defect is present. Upon respiratory correction, the LV is improved in uniformity in both MCR and PMC. This is likely the reason for the improved defect detection results by the two algorithms in the ROC studies.

The FWHM results indicate that the reconstructed images with respiratory correction also exhibited improved spatial resolution in the LV. While the Gaussian filter with increased smoothing could potentially override the effect of respiratory motion correction, it is noted that at a given dose level, the obtained FWHM values were always smaller with motion correction than without (Figure 3). At full dose, despite more post-filtering being applied for MCR and PMC than for Non-MC at optimal AUC settings, MCR and PMC still yielded smaller FWHM values (2.13 and 2.29 cm, respectively) than Non-MC (2.23 cm). The FWHM values of the reconstructed LV are noted to increase with reduced dose level, but the improvement by MCR becomes more pronounced at lower dose. For example, at 12.5% dose, the FWHM is 2.40 cm for MCR vs 2.58 cm for Non-MC.

The perfusion images of patient #1 (Figures 4 and 6) are noted to have better separation of the inferior LV

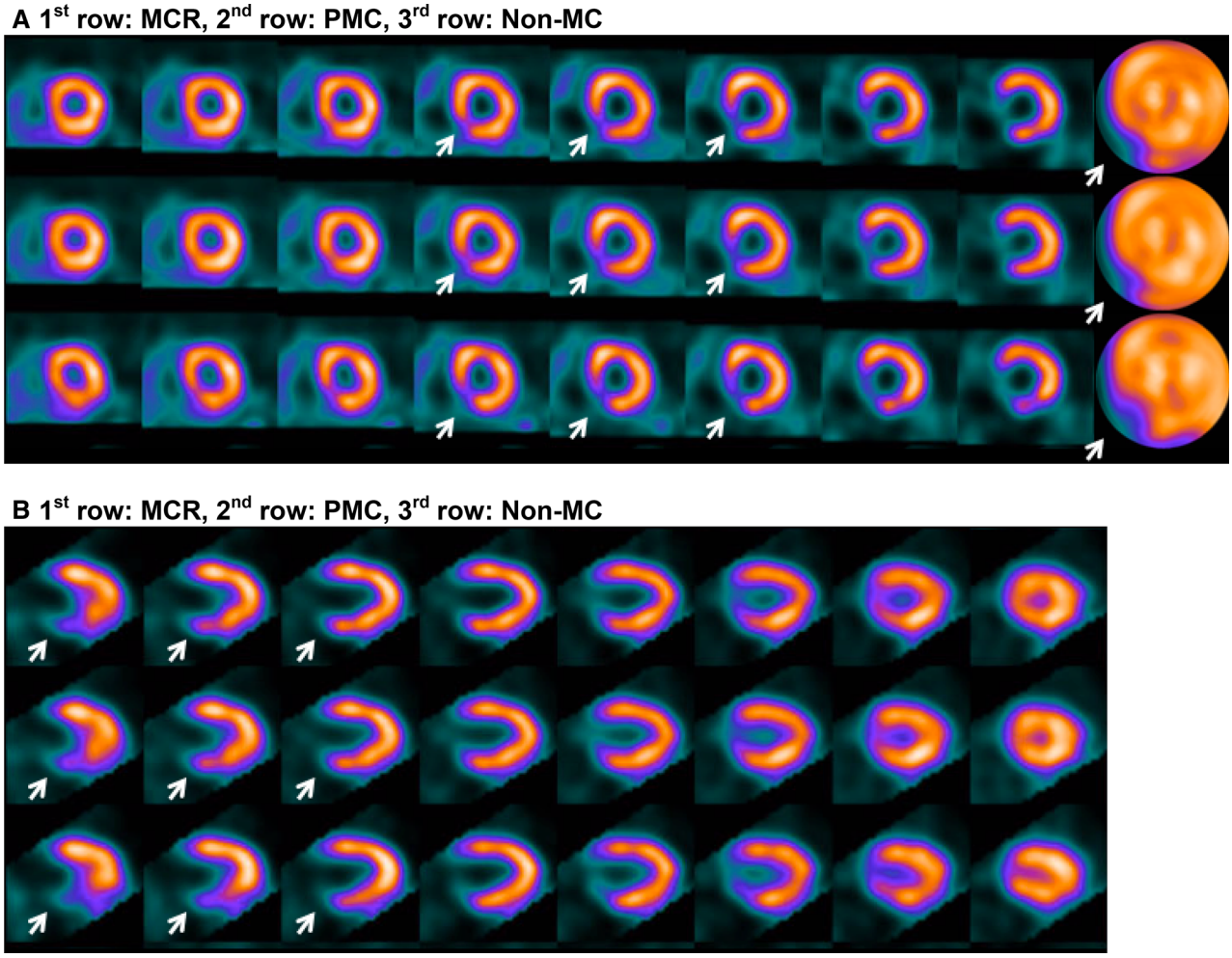

Figure 7. Reconstructed images of subject #2 (same as Figure 5) at 12.5% dose. The regional cooling away from the defect in the inferior LV wall observed in Non-MC is improved by respiratory motion correction in MCR and PMC.

wall from sub-diaphragmatic activity upon respiratory motion correction. This was also observed in a number of other patients in the dataset. This benefit was also reported in previous studies.[36,37]

In the experiments the center bin based on the amplitude of the superoinferior motion was used as the reference bin for reconstruction. Alternatively, when MCR is used, it might be more beneficial to use the end-expiration bin as the reference, because its imaging time is likely longer and hence in better alignment with the attenuation map. However, when PMC is used, it won't make any difference because the individual bins were reconstructed independently with the same attenuation map.

Finally, in the experiments, we used the BSREM algorithm for ML image reconstruction. However, the optimal AUC values obtained in Non-MC at various dose levels are nearly identical to the results previously reported in Ref. 26 where OSEM was used for traditional acquisitions. This indicates that the reported results here should be applicable to OSEM reconstruction as well.

CONCLUSIONS

We investigated quantitatively the potential benefit of respiratory-binned acquisitions in SPECT imaging in terms of (1) detectability of perfusion defects and (2) spatial resolution of the LV wall. Both at full dose and at reduced dose, motion correction could achieve higher perfusion defect detection accuracy over traditional reconstruction. Motion-compensated reconstruction (MCR) could yield more accurate results than post-reconstruction motion correction (PMC). Similar improvements were also obtained in the LV resolution

with motion correction. Improved perfusion uniformity in the reconstructed LV was also observed with motion correction at all dose levels.

NEW KNOWLEDGE GAINED

Our work demonstrates the potentially positive benefit of respiratory correction in image reconstruction for SPECT-MPI both at standard dose and at reduced dose. Both motion-compensated reconstruction and post-reconstruction correction can improve the image accuracy and detection performance of perfusion defects over traditional data acquisitions. Motion correction can contribute to achieving further dose reduction while maintaining the diagnostic accuracy in traditional reconstruction.

Acknowledgements

This work was supported by the National Institutes of Health (NIH) Grant R01-HL122484. P.S. was also supported by NIH Grant R01-HL089765. The content is solely the responsibility of the authors and does not necessarily represent the official views of the NIH.

Disclosure

The University of Massachusetts (Michael A. King, P. Hendrik Pretorius, and Karen L. Johnson) had a research agreement with Philips Healthcare at the time some of this work was performed. Chao Song, Yongyi Yang, Albert Juan Ramon, Miles N. Wernick, and Piotr J. Slomka have nothing to disclose.

References

1. DePuey EG. Garcia. Updated imaging guidelines for nuclear cardiology procedures part I. J Nucl Cardiol. 2001;8:G5-58.
2. Lin GS, Hines HH, Grant G, Taylor K, Ryals C. Automated quantification of myocardial ischemia and wall motion defects by use of cardiac SPECT polar mapping and 4-dimensional surface rendering. J Nucl Med Technol. 2006;34:3-17.
3. Arsanjani R, Xu Y, Hayes SW, Fish M, Lemley M, Gerlach J, Dorbala S, Berman DS, Germano G, Slomka P. Comparison of fully automated computer analysis and visual scoring for detection of coronary artery disease from myocardial perfusion SPECT in a large population. J Nucl Med. 2013;54:221-8.
4. Slomka PJ, Nishina H, Berman DS, Akincioglu C, Abidov A, Friedman JD, Hayes SW, Germano G. Automated quantification of myocardium perfusion SPECT using simplified normal limits. J Nucl Cardiol. 2005;12:66-77.
5. Cooper JA, Neumann PH, McCandless BK. Effect of patient motion on tomographic myocardial perfusion imaging. J Nucl Med. 1992;33:1566-71.
6. Segars WP, Tsui BM. Study of the efficacy of respiratory gating in myocardial SPECT using the new 4-D NCAT phantom. IEEE Trans Nucl Sci. 2002;49:675-9.
7. Kovalski G, Israel O, Keidar Z, Frenkel A, Sachs J, Azhari H. Correction of heart motion due to respiration in clinical myocardial perfusion SPECT scans using respiratory gating. J Nucl Med. 2007;48:630-6.
8. Murase K, Ishine M, Kataoka M, Itoh H, Mogami H, Lio A, Hamamoto K. Simulation and experimental study of respiratory motion effect on image quality of single photon emission computed tomography (SPECT). Eur J Nucl Med Mol Imaging. 1987;12:244-9.
9. Tsui BM, Segars WP, Lalush DS. Effects of upward creep and respiratory motion in myocardial SPECT. IEEE Trans Nucl Sci. 2000;47:1192-5.
10. Dasari PK, Konik A, Pretorius PH, Johnson KL, Segars WP, Shazeeb MS, King MA. Correction of hysteretic respiratory motion in SPECT myocardial perfusion imaging: Simulation and patient studies. Med Phys. 2017;44:437-50.
11. Cho K, Kumiata SI, Okada S, Kumazaki T. Development of respiratory gated myocardial SPECT system. J Nucl Cardiol. 1999;6:20-8.
12. Parker JG, Mair BA, Gilland DR. Respiratory motion correction in gated cardiac SPECT using quaternion-based, rigid-body registration. Med Phys. 2009;36:4742-54.
13. Lu W, Parikh PJ, Hubenschmidt JP, Bradley JD, Low DA. A comparison between amplitude sorting and phase-angle sorting using external respiratory measurement for 4D CT. Med Phys. 2006;33:2964-74.
14. Dey J, Segars WP, Pretorius PH, Walvick RP, Bruyant PP, Dahlberg S, King MA. Estimation and correction of cardiac respiratory motion in SPECT in the presence of limited-angle effects due to irregular respiration. Med Phys. 2010;37:6453-65.
15. Qi W, Yang Y, Wernick MN, Pretorius PH, King MA. Limited-angle effect compensation for respiratory binned cardiac SPECT. Med Phys. 2016;43:443-54.
16. Pretorius PH, Johnson KL, Dahlberg ST, King MA. Investigation of the physical effects of respiratory motion compensation in a large population of patients undergoing Tc-99m cardiac perfusion SPECT/CT stress imaging. J Nucl Cardiol. 2017. https://doi.org/10.1007/s12350-017-0890.
17. Song C, Yang Y, Qi W, Wernick M, Pretorius PH, King MA. Motion-compensated image reconstruction vs post-reconstruction correction in respiratory-binned SPECT with standard and reduced dose acquisitions. Med Phys. 2018;45(7):2991-3000.
18. Hamann M, Aldridge M, Dickson J, Endozo R, Lozhkin K, Hutton BF. Evaluation of a low-dose/slow-rotating SPECT-CT system. Phys Med Biol. 2008;53:2495.
19. Jin M, Niu X, Qi W, Yang Y, Dey J, King MA, Dahlberg S, Wernick MN. 4D reconstruction for low-dose cardiac gated SPECT. Med Phys. 2013;40:022501.
20. Song C, Yang Y, Wernick MN, Pretorius PH, King MA. Optimizing motion correction in reconstruction of respiratory-gated SPECT. In Biomedical Imaging (ISBI), 2016 IEEE; 2016. p. 36-39.
21. Slomka P, Germano G. "Optimizing radiation dose and imaging time with conventional myocardial perfusion SPECT: Technical aspects. J Nucl Cardiol. 2017;24:888-91.
22. Mattsson S, Soderberg M. Radiation dose management in CT, SPECT/CT and PET/CT techniques. Radiat Prot Dosimetry. 2011;147:13-21.
23. Duvall WL, Tandon TS, Henzlova MJ. The time is now: Dose reduction for myocardium perfusion imaging. J Nucl Cardiol. 2018;25:131-3.
24. van Dijk JD, Borren NM, Mouden M, van Dalen JA, Ottervanger JP, Jager PL. Effect of a patient-specific minimum activity in stress myocardial perfusion imaging using CZT-SPECT:

Prognostic value, radiation dose, and scan outcome. J Nucl Cardiol. 2018;25:26-35.
25. Verberne HJ, Scholtens AM. The very hungry caterpillar and the ongoing effort to reduce radiation in myocardial perfusion scintigraphy: Have we become the beautiful butterfly? J Nucl Cardiol. 2018;25:36-8.
26. Ramon AJ, Yang Y, Pretorius PH, Slomka PJ, Johnson KL, King MA, Wernick MN. Investigation of dose reduction in cardiac perfusion SPECT via optimization and choice of the image reconstruction strategy. J Nucl Cardiol. 2017. https://doi.org/10.1007/s12350-017-0920-1.
27. Pretorius PH, King MA, Johnson K, Yang Y, Wernick MN. Evaluating the effect of incremental dose reduction on perfusion defect detection employing hybrid cardiac perfusion SPECT slices. In Nuclear Science Symposium and Medical Imaging Conference 2015; 1-4.
28. Svane B, Bone D, Holmgren A, Landou C. Polar presentation of coronary angiography and thallium-201 single photon emission computed tomography: A method for comparing anatomic and pathologic findings in coronary angiography with isotope distribution in thallium-201 myocardial SPECT. Acta Radiol. 1989;30:561-74.
29. King MA, Pan TS, Pretorius PH, Case JA. An investigation of the filtering of TEW scatter estimates used to compensate for scatter with ordered subset reconstruction. IEEE Trans Nucl Sci. 1997;44:1140-5.
30. Ahn S, Fessler JA. Globally convergent image reconstruction for emission tomography using relaxed ordered subsets algorithms. IEEE Trans Med Imaging. 2003;22:613-26.
31. Sah BR, Stolzmann P, Delso G, Wollenweber SD, Hullner M, Hakami YA, Queiroz MA, Barbosa FG, von Schulthess GK, Pietsch C, Veit-Haibach P. Clinical evaluation of a block sequential regularized expectation maximization reconstruction algorithm in 18F-FDG PET/CT studies. Nucl Med Commun. 2017;38:57-66.
32. Maintz JA, Viergever MA. A survey of medical image registration. Med Image Anal. 1998;2:1-36.
33. Metz C, Lorenzo LP, Papaioannu J. ROC-kit software. http://metz-roc.uchicago.edu/MetzROC/software; 2011.
34. Qi W, Yang Y, Song C, Wernick MN, Pretorius MN, King MA. 4-D reconstruction with respiratory correction for gated myocardial perfusion SPECT. IEEE Trans Med Imaging. 2017;36:1626-35.
35. Valenta I, Treyer V, Husmann L, Gaemperli O, Schindler MJ, Herzog BA, et al. New reconstruction algorithm allows shortened acquisition time for myocardial perfusion SPECT. Eur J Nucl Med Mol Imaging. 2010;37:750-7.
36. Narayanan MV, King MA, et al. Human-observer receiver-operating-characteristic evaluation of attenuation, scatter, and resolution compensation strategies for ^{99m}TC myocardial perfusion imaging. J Nucl Med. 2003;44(11):1725-34.
37. Pitman AG, Kalff V, van Every B, Risa B, Barnden LR, Kelly MJ. Contributions of subdiaphragmatic activity, attenuation, and diaphragmatic motion to inferior wall artifact in attenuation-correction Tc-99m myocardial perfusion SPECT. J Nucl Cardiol. 2002;12(4):401-9.